Proceedings of Meetings on Acoustics

ICA 2013 Montreal
Montreal, Canada
2 - 7 June 2013

Architectural Acoustics

Session 5aAAb: Effects of Room Boundaries on Diffusion and Reverberation

5aAAb1.   Energy decay analysis of non-diffuse sound fields in rectangular rooms

Tetsuya Sakuma* and Kazushi Eda

 *Corresponding author's address: University of Tokyo, Kashiwa, 2778563, Chiba, Japan, sakuma@k.u-tokyo.ac.jp

  Rectangular rooms with irregular aspect ratio or nonuniform absorption distribution apt to have non-diffuse sound fields, where the curvature of energy decay curve occurs in the reverberation process. In general, this curvature leads to longer reverberation times than the estimates by the Sabine or Eyring formula; however it can be suppressed to a certain extent with diffusive wall surfaces. Recently the author has proposed a new approximate theory of reverberation in rectangular rooms with specular and diffuse reflections. In this paper, the validity of the theory is investigated by two case studies with geometrical and wave-based acoustic simulation. In the first study, energy decay in a variety of rectangular rooms with changing the aspect ratio, the absorption distribution and the scattering coefficient, is simulated with the image source method and the ray tracing method. In the second study, a two-dimensional FDTD analysis is performed to demonstrate the frequency dependence of energy decay in a variety of rectangular rooms with flat or corrugated walls. Finally, the simulated results are compared with the theoretical ones, and the validity and the limitation of the approximation are discussed.

1. INTRODUCTION

It is well known that rectangular rooms with irregular aspect ratio or nonuniform absorption distribution apt to have non-diffuse sound fields. In such rooms, curvature occurs in energy decay curve, which leads to longer reverberation times than the estimates by the Sabine or Eyring formula. However the curvature can be suppressed to a certain extent by installing diffusive wall surfaces.

Recently the author has proposed a new approximate theory of reverberation in rectangular rooms with specular and diffuse reflections [1]. In this paper, the validity of the theory is investigated by two case studies with geometrical and wave-based acoustic simulation. In the first study, energy decay curves in a variety of rectangular rooms, changing the aspect ratio, the absorption distribution and the scattering coefficient, are simulated with the image source method and the ray tracing method. In the second study, a two-dimensional FDTD analysis is performed to demonstrate the frequency dependence of energy decay curve for a variety of rectangular rooms with flat or corrugated walls. Finally, simulated results are compared with theoretical ones, and the validity and limitation of the approximation are discussed.

2. APPROXIMATE THEORY OF REVERBERATION

A variety of theories of reverberation in rooms have been proposed, originated from Sabine's formula on the assumption of perfectly diffuse field, modified by Eyring-Norris, Millington-Sette, Kuttruff and others. For rectangular rooms, an empirical formula was first proposed by Fitzroy [2], and followed by Pujolle [3], Hirata [4], Arau-Puchades [5], Nilsson [6], Neubauer [7] and others. However, no theory has been established that considers different effects of specular and diffuse reflections on reverberation. The author has recently developed an approximate theory for rectangular rooms based on the image source method, where a sound field is supposed to be divided into specular and diffuse fields by employing scattering coefficients [8] of wall surfaces. The outline of the theory is described below.

2.1. Reverberation of Specular Field in a Rectangular Room

In a grid arrangement of image sources for a rectangular room, they are divided into axial, tangential and oblique groups, which chiefly contribute to the corresponding groups of normal modes in wave acoustics. The critical angles for grouping in three directions are frequency-dependently given by $\theta_{x(y,z)} = \pi c / 2\omega L_{x(y,z)}$, with the length of each side $L_{x(y,z)}$ (Figure 1). Assuming that energy decay of each group is exponential, reverberation of the total specular field is composed of seven kinds of exponential decay, as follows.

$$E^{S}(t) = \frac{W}{c}\left[\frac{\gamma_{ob}}{\hat{A}_{ob}}\exp\left(-\frac{\hat{A}_{ob}ct}{V} \right) + \sum_{xy}\frac{2\gamma_{txy}}{\hat{A}_{txy}}\exp\left(-\frac{\hat{A}_{txy}ct}{V} \right) + \sum_{x}\frac{4\gamma_{ax}}{\hat{A}_{ax}}\exp\left(-\frac{\hat{A}_{ax}ct}{V} \right) \right], \tag{1}$$

where the proportion of sources in each group is denoted by

$$\gamma_{ob} = 1 - \frac{\pi c S}{4\omega V} + \frac{\pi c^2 L}{8\omega^2 V}, \quad \gamma_{txy} = \frac{\pi c L_x L_y}{2\omega V}\left[1 - \frac{c\left(L_x + L_y \right)}{\omega L_x L_y} \right], \quad \gamma_{ax} = \frac{\pi c^2 L_x}{2\omega^2 V}, \tag{2}$$

with the room volume $V = L_x L_y L_z$, the total surface area $S = 2\left(L_x L_y + L_y L_z + L_z L_x \right)$, and the total edge length $L = 4\left(L_x + L_y + L_z \right)$.

Regarding absorption factors, $\hat{A}_{ob} = A_{ob}/4$, $\hat{A}_{txy} = A_{txy}/\pi$, and $\hat{A}_{ax} = A_{ax}/2$; $A_{ob} = S\alpha_{Eob}$, $A_{txy} = 2\left(L_x + L_y \right)L_z\alpha_{Etxy}$, and $A_{ax} = 2L_y L_z\alpha_{Eax}$; $\alpha_{Eob(txy,ar)} = -\ln\left(1 - \alpha_{ob(txy,ar)} \right)$; $\alpha_{ob(txy,ar)}$ is the average absorption coefficient for each group, which is given by geometric mean in each direction, due to alternative reflections between parallel walls. Additionally, for axial and tangential groups, special averaging is given by taking into account the reflection frequency in each direction, as a function of the critical angles. In axial or tangential directions, normal or random incidence values are used for the greater part of reflections, whereas grazing

incidence values are used for few reflections in off-axial off-tangential directions. Furthermore, diffusivity of wall surfaces can be considered by replacing all values related to absorption coefficient with those related to specular absorption coefficient, $\beta = \alpha + (1-\alpha)s$, with scattering coefficient s. Accordingly, Equation (1) is simply modified by substituting $\left(\beta, \beta_\mathrm{E}, B, \hat{B}\right)$ for $\left(\alpha, \alpha_\mathrm{E}, A, \hat{A}\right)$.
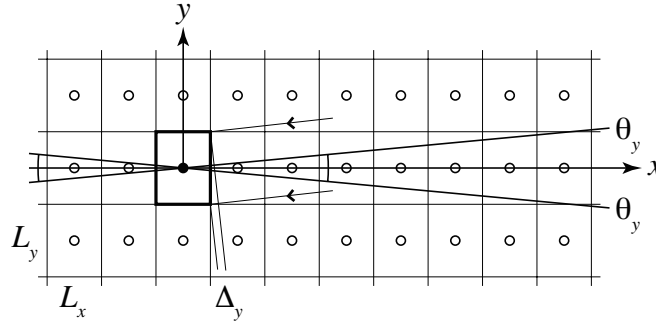

FIGURE 1. Axial image sources for the *x*-axis in the *xy*-plane.

2.2. Reverberation of Diffuse Field in a Rectangular Room

By the scattering coefficients of wall surfaces, sound energy propagating from image sources is divided into specular and diffuse components at each reflection. It seems reasonable that a specular field is composed of arriving components that are never scattered at all reflections from image sources to a receiving point. Therefore, as illustrated in Figure 2, it is assumed that a part of specular energy is transformed into diffuse energy at each refection, and after the transition, the diffuse energy is decayed by perfectly diffuse reflections and finally arrives to a receiving point by random incidence. Considering the transition from specular energy of each source group, energy density of the total diffuse field is expressed by

$$E^\mathrm{D}(t) = \frac{W}{c}\left[\frac{\mu_\mathrm{r}}{\hat{A}_\mathrm{r}}\exp\left(-\frac{\hat{A}_\mathrm{r}ct}{V}\right) - \frac{\gamma_\mathrm{ob}\mu_\mathrm{ob}}{\hat{B}_\mathrm{ob}}\exp\left(-\frac{\hat{B}_\mathrm{ob}ct}{V}\right) - \sum_{xy}\frac{\gamma_\mathrm{txy}\mu_\mathrm{txy}}{\hat{B}_\mathrm{txy}}\exp\left(-\frac{\hat{B}_\mathrm{txy}ct}{V}\right) - \sum_{x}\frac{\gamma_\mathrm{ax}\mu_\mathrm{ax}}{\hat{B}_\mathrm{ax}}\exp\left(-\frac{\hat{B}_\mathrm{ax}ct}{V}\right)\right], \qquad (3)$$

where $\mu_\mathrm{r} = \gamma_\mathrm{ob}\mu_\mathrm{ob} + \sum_{xy}\gamma_\mathrm{txy}\mu_\mathrm{txy} + \sum_x\gamma_\mathrm{ax}\mu_\mathrm{ax}$; $\mu_\mathrm{ob(txy,ax)} = \hat{S}_\mathrm{ob(txy,ax)}\big/\left(\hat{B}_\mathrm{ob(txy,ax)} - \hat{A}_\mathrm{r}\right)$, with $\hat{A}_\mathrm{r}$ for the ordinary average random-incidence absorption coefficient. In a similar way to absorption coefficient, $\hat{S}_\mathrm{ob} = S_\mathrm{ob}/4$, $\hat{S}_\mathrm{txy} = S_\mathrm{txy}/\pi$, and $\hat{S}_\mathrm{ax} = S_\mathrm{ax}/2$; $S_\mathrm{ob} = Ss_\mathrm{Eob}$, $S_\mathrm{txy} = 2\left(L_x + L_y\right)L_z s_\mathrm{Etxy}$, and $S_\mathrm{ax} = 2L_y L_z s_\mathrm{Eax}$; $s_\mathrm{Eob(txy,ax)} = -\ln\left(1 - s_\mathrm{ob(txy,ax)}\right)$; $s_\mathrm{ob(txy,ax)}$ is the average scattering coefficient for each group.

Consequently, as the sum of specular and diffuse fields, the overall energy density is apparently composed of eight kinds of exponential decay, as follows:

$$E(t) = E^\mathrm{S}(t) + E^\mathrm{D}(t) = \frac{W}{c}\left[\frac{\mu_\mathrm{r}}{\hat{A}_\mathrm{r}}\exp\left(-\frac{\hat{A}_\mathrm{r}ct}{V}\right) + \frac{\gamma_\mathrm{ob}\left(1 - \mu_\mathrm{ob}\right)}{\hat{B}_\mathrm{ob}}\exp\left(-\frac{\hat{B}_\mathrm{ob}ct}{V}\right)\right.$$
$$\left. + \sum_{xy}\frac{\gamma_\mathrm{txy}\left(2 - \mu_\mathrm{txy}\right)}{\hat{B}_\mathrm{txy}}\exp\left(-\frac{\hat{B}_\mathrm{txy}ct}{V}\right) + \sum_x\frac{\gamma_\mathrm{ax}\left(4 - \mu_\mathrm{ax}\right)}{\hat{B}_\mathrm{ax}}\exp\left(-\frac{\hat{B}_\mathrm{ax}ct}{V}\right)\right], \qquad (4)$$

where the decay rates correspond to seven rates for the specular fields, and one rate for the diffuse field. Each decay rate is given by

$$\left(D^\mathrm{S}_\mathrm{ax} \ D^\mathrm{S}_\mathrm{ay} \ D^\mathrm{S}_\mathrm{az} \Big| D^\mathrm{S}_\mathrm{txy} \ D^\mathrm{S}_\mathrm{tyz} \ D^\mathrm{S}_\mathrm{tzx} \Big| D^\mathrm{S}_\mathrm{ob} \Big| D^\mathrm{D}_\mathrm{r}\right) = 10\log_{10}\mathrm{e}\frac{c}{V}\left(\hat{B}_\mathrm{ax} \ \hat{B}_\mathrm{ay} \ \hat{B}_\mathrm{az} \Big| \hat{B}_\mathrm{txy} \ \hat{B}_\mathrm{tyz} \ \hat{B}_\mathrm{tzx} \Big| \hat{B}_\mathrm{ob} \Big| \hat{A}_\mathrm{r}\right), \qquad (5)$$

with the relations, $\min\left(D^\mathrm{S}_\mathrm{ax}, D^\mathrm{S}_\mathrm{ay}, D^\mathrm{S}_\mathrm{az}\right) < \min\left(D^\mathrm{S}_\mathrm{txy}, D^\mathrm{S}_\mathrm{tyz}, D^\mathrm{S}_\mathrm{tzx}\right) < D^\mathrm{S}_\mathrm{ob}$, and $D^\mathrm{D}_\mathrm{r} \leq D^\mathrm{S}_\mathrm{ob}$.
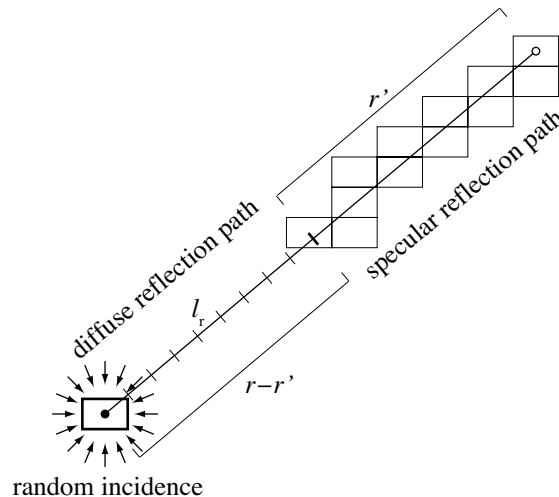
FIGURE 2. Transition from specular to diffuse reflections.

3. GEOMETRIC SIMULATION OF REVERBERATION

In order to validate the approximate theory, two kinds of geometric simulation are conducted. Firstly, specular fields without diffusive walls are simulated by the image source method; secondly, specular/diffuse mixed fields with diffusive walls are simulated by the ray tracing method. As shown in Table 1, four types of rectangular rooms have an equal volume 1,000 m³, and an equal absorption area 210 m², but different aspect ratios and absorption distributions. In all cases, the Sabine's reverberation times are 0.77 s, and absorption and scattering coefficients are assumed to have no incidence-angle dependence.

TABLE 1. Conditions of rectangular rooms.

Case	L_x (m)	L_y (m)	L_z (m)	α_x	α_y	α_z	Ratio of α/L
1a	10	10	10	0.35	0.35	0.35	1:1:1
1b	10	10	10	0.15	0.30	0.60	1:2:4
2a	20	10	5	0.30	0.30	0.30	1:2:4
2b	20	10	5	0.10	0.20	0.40	1:4:16

3.1. Specular Field Simulated with the Image Source Method

In the simulation with the image source method, a continuous uniform distribution of sources is assumed in the rooms. Figure 3 shows energy decay curves of seven image source groups and the total for Case 1a (cube, uniform absorption) and Case 2b (non-cube, nonuniform absorption), calculated by the image source method and the approximate theory. In Case 1a, decay lines are almost straight, and the total slope estimated by the theory becomes slightly gentle at the low frequency. In Case 2b, total decay lines are clearly curved, especially in the theoretical line at the high frequency, rather apart from the geometrically simulated. In the theory, a straight decay line is assumed for each group, whereas a curved line appears for the oblique group in the geometric simulation. It seems that the theory cannot estimate energy density of the oblique group in the late decay. On the other hand, the theory possibly estimates gentle slopes of axial and tangential group, which are dominant in the late decay.

3.2. Specular/Diffuse Mixed Field Simulated with the Ray Tracing Method

The classical ray tracing method is applied with taking into account scattering coefficients of wall surfaces. A sound ray is stochastically determined to be specularly or randomly directed at each reflection, and once randomly reflected, the ray repeats it according to Lambert's law. The number of rays is 10⁶, the area of a receiving sphere is 1m², and a uniform scattering coefficient, from 0.05 to 0.8, is given to all wall surfaces in

the four cases. Figure 4 shows overall energy decay curves of the specular/diffuse mixed field, calculated by the ray tracing method and the approximate theory at 125 Hz. In Case 1a, surface scattering does not affect the overall decay, but remarkably does in the other cases. It is seen that, with increasing the scattering coefficient, the decay slope steadily becomes steeper to approach the Eyring's slope, suppressing its curvature. However, a change of scattering coefficient from 0.4 to 0.8 hardly affects the total decay in all cases. In these general tendencies, good agreement is seen between the ray tracing method and the theory.
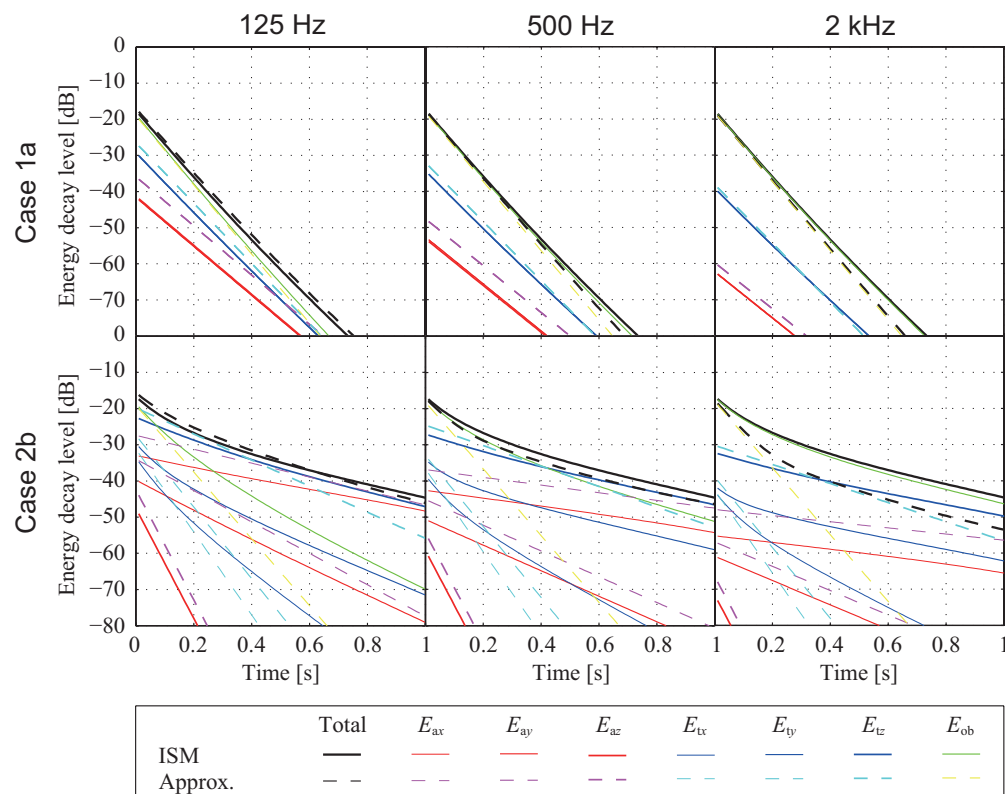
FIGURE 3. Energy decay curves of seven image source groups and the total, calculated by the image source method and the approximate theory. Upper: Case 1a; Lower: Case 2b, at 125, 500 and 2 kHz.
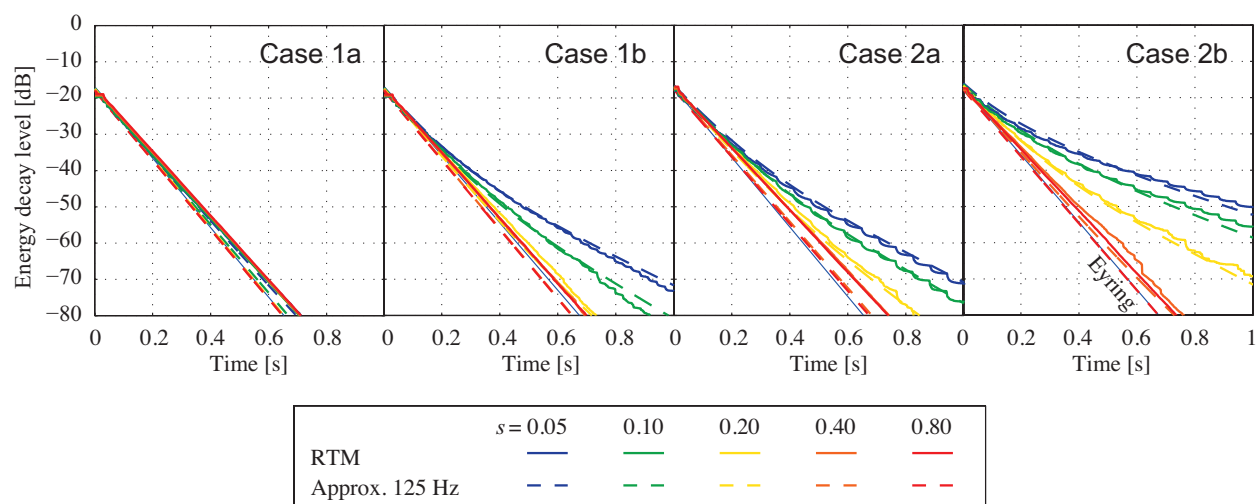

FIGURE 4. Energy decay curves of the overall field with changing the scattering coefficient of walls, calculated by the ray tracing method and the approximate theory at 125 Hz.

4. TWO-DIMENSIONAL WAVE-BASED SIMULATION OF REVERBERATION

In order to investigate realistic reverberation in non-diffuse sound fields, wave-based simulation is conducted using the finite-difference time-domain (FDTD) method in two-dimensional rectangular rooms. Figure 5 illustrates room geometry, arrangement of a source and receiving points, and three types of x-directional walls in a combination of flat and diffusive walls. Table 2 shows a variation of room conditions, in a combination of four cases and three wall types. All walls are reflective in Case O, whereas y-directional walls are absorptive in the other cases with different aspect ratios. Diffusive walls for x-direction have square blocks of a side length of 100 mm, spaced at a pitch of 200 mm, and of which random/normal -incidence scattering coefficients are given by numerical analysis [9] as shown in Figure 6.

TABLE 2. Conditions of two-dimensional rectangular rooms.

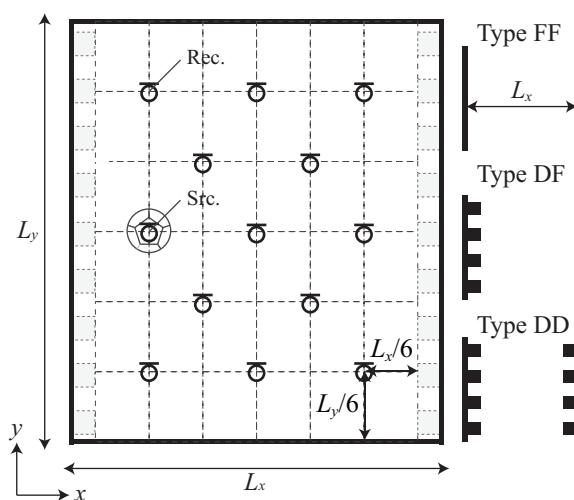| Case	L_x (m)	L_y (m)	α^n_x	α^n_y	Wall Type
O	8	8	0.05	0.05	FF / DF / DD
A	4	16	0.05	0.80	FF / DF / DD
B	8	8	0.05	0.80	FF / DF / DD
C	16	4	0.05	0.80	FF / DF / DD

FIGURE 5. Arrangement of a source and receiving points, and three types of x-directional walls. Diffusive walls have square blocks of a side length of 100 mm, spaced at a pitch of 200 mm.
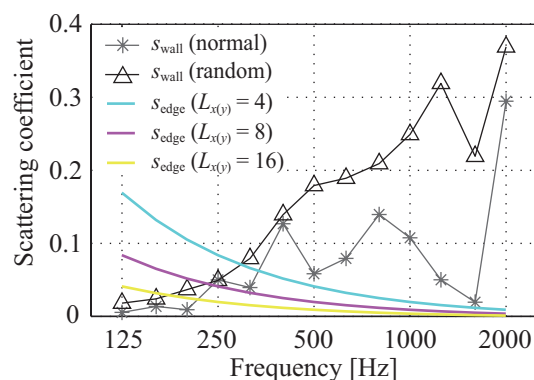

FIGURE 6. Normal/random-incidence scattering coefficients of the x-directional diffusive wall, and additional scattering coefficients for the walls of three different widths.

4.1. Inclusion of Edge Scattering in Theoretical Approximation

According to the approximate theory, a sound field in a two-dimensional rectangular room is composed of three kinds of specular fields (oblique and two axial) and a diffuse field, thus assuming four kinds of exponential decay. In the theoretical approximation, random/normal/grazing-incidence absorption coefficients are given by averaging directional coefficients over the corresponding angle ranges: overall, 0 to the critical angle, and the critical angle to 90 degrees, respectively. Random/normal-scattering coefficients are given as shown in Figure 6, and grazing-incidence scattering coefficient is assumed to be 0.

It is expected that edge scattering occurs on the periphery of a wall, therefore the additional scattering coefficient is often taken into account in geometric simulation [10]. In a two-dimensional room, the additional scattering coefficient for both sides of a wall is assumed to be given by

$$s_{\mathrm{edge}} = 0.5 \times 2 l_{\mathrm{edge}} / L_{x(y)}, \qquad (6)$$

where $l_{\mathrm{edge}} = \lambda/4$. Consequently, the effective scattering coefficient of the wall is given by $s_{\mathrm{eff}} = s_{\mathrm{surf}} + s_{\mathrm{edge}}$, if $s_{\mathrm{eff}} < 1$; otherwise $s_{\mathrm{eff}} = 1$. For the walls of three different widths, the additional scattering coefficients are shown in Figure 6.

4.2. Two-Dimensional FDTD Simulation

In the FDTD simulation, a real part of impedance is given as boundary condition, corresponding to the normal-incidence absorption coefficient in Table 2. As source condition, a Gaussian spatial distribution is given, which contains sufficient energy below 2.5 kHz. After the simulation, the obtained responses are filtered into 1/3 octave bands, and average energy decay over 13 receiving points is calculated in each band. Finally, in a specific range of decay, reverberation times are determined by the least squares regression.

Figure 7 shows energy decay curves for Type FF (with flat walls), calculated by the FDTD method and the approximate theory with and without considering edge scattering. In Case O, decay lines are almost straight, corresponding to the Eyring's slope independently of frequency band. In the other cases, the slope becomes gentle in the high frequency band, and the tendency is more remarkable as increasing the distance between *x*-directional walls. Similar tendencies are seen in the theoretical results, however there are considerable discrepancies from the numerical results. Including edge scattering in the theoretical approximation, the discrepancies seem to be somewhat smaller in all cases.

Figure 8 shows reverberation times determined in the decay range of -5 to -35 dB, for three wall types in each case. In the numerical results except for Cases O, reverberation times for Type FF are longer up to the one-dimensional Eyring's value at higher frequencies, and the tendency is more remarkable as increasing the distance between *x*-directional walls. For Types DF and DD with diffusive walls, the reverberation times become shorter, corresponding to the frequency characteristics of normal-incidence scattering coefficient. These tendencies are roughly seen in the theoretical results, where inclusion of edge scattering is necessary at low frequencies. The agreement between theoretical and numerical results is relatively well in Case B (square), however it depends on the aspect ratio of the room. One peculiar behavior is observed in Case O with Type DD, where remarkable discrepancies from the two-dimensional Eyring's value occur in the numerical results. It probably means that energy scattered by the *x*-directional diffusive walls is transformed into specular energy in the *y*-directional axial field. This reversible transition from diffuse to specular energy is not considered in the approximate theory.
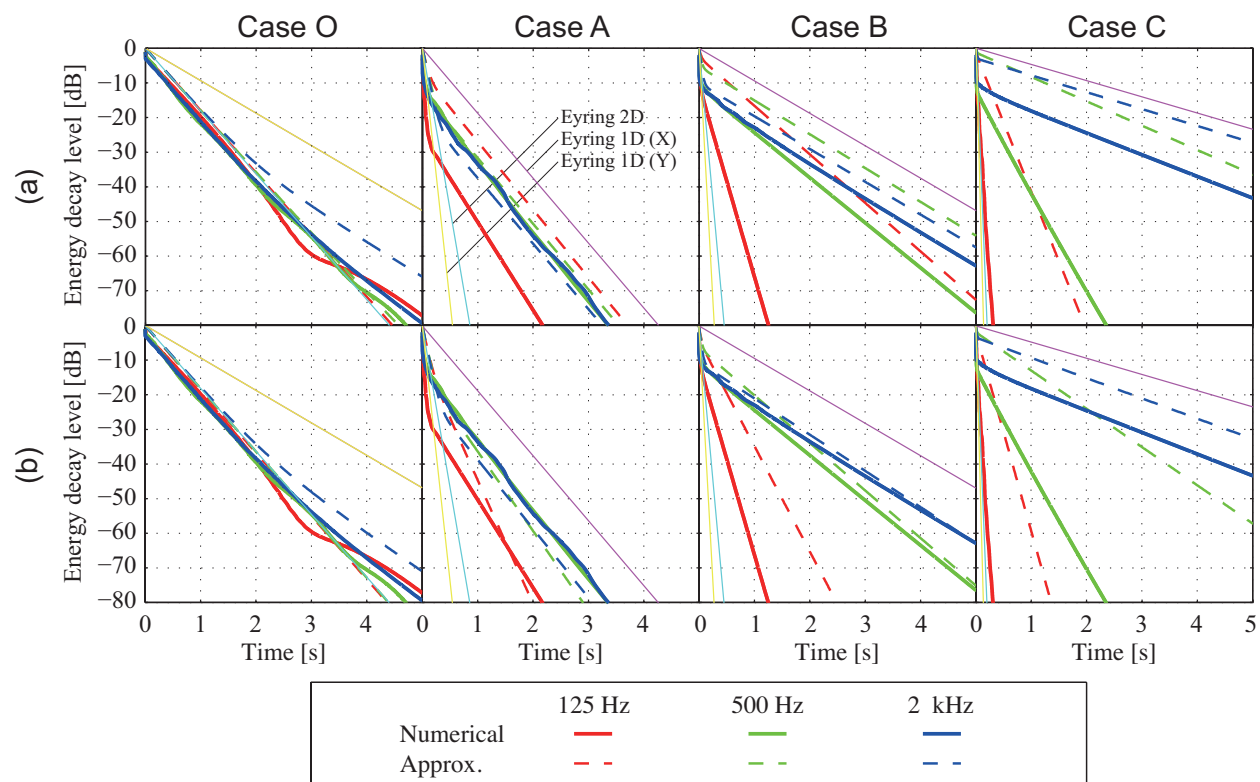
FIGURE 7. Energy decay curves for Type FF in 1/3 octave bands of 125, 500 and 2 kHz, calculated by the FDTD method and the approximate theory: (a) without edge scattering, (b) with edge scattering.
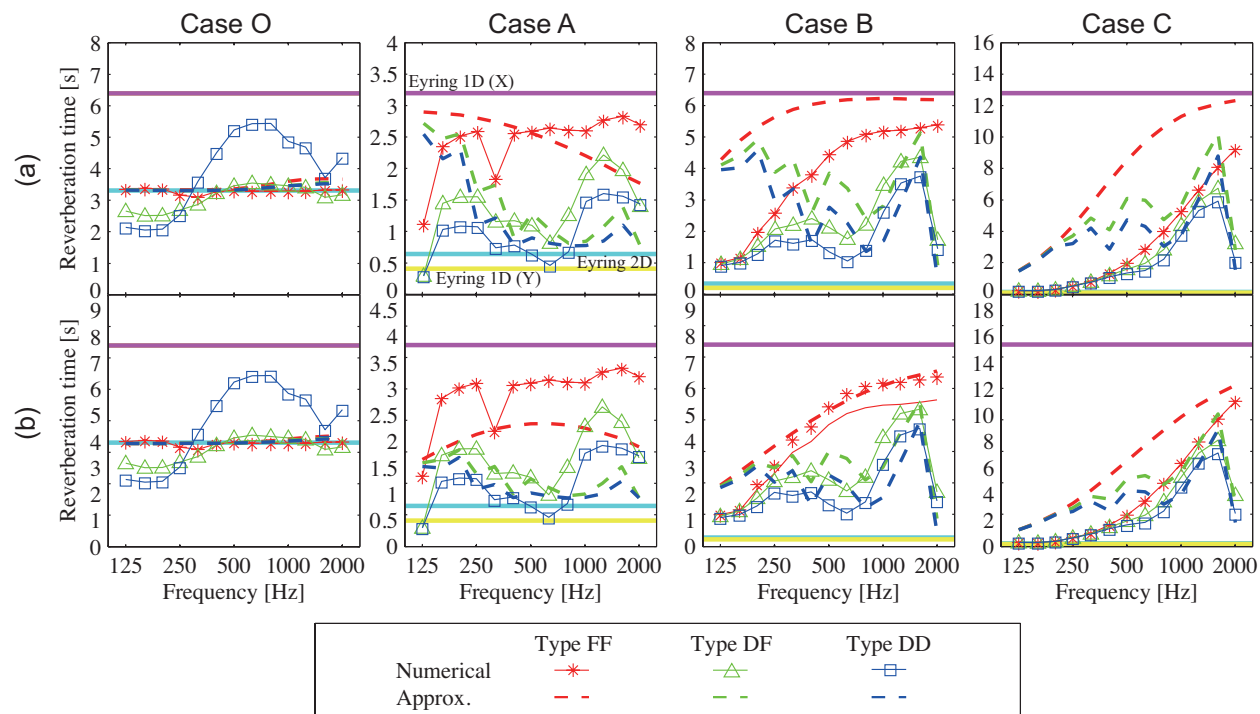

FIGURE 8. Reverberation times T_{30} (-5 to -35 dB), calculated by the FDTD method and the approximate theory: (a) without edge scattering, (b) with edge scattering.

CONCLUSION

Reverberation of non-diffuse sound fields in a variety of rectangular rooms is simulated with geometrical and wave-based acoustic simulation, and the validity of the approximate theory is investigated.

In the comparison with geometrical simulation, the theory can fairly well estimate overall energy decay curves in various conditions changing room aspect ratio, absorption distribution and scattering coefficients of wall surfaces; however, it cannot accurately estimate energy decay of each source group, especially for the oblique group in the late decay.

In the comparison with two-dimensional wave-based simulation, the theory can roughly estimate frequency characteristics of reverberation time, provided that edge scattering is included at low frequencies. The agreement is relatively well in a square room, however it depends on room aspect ratio. The treatment of edge scattering is to be further investigated in relation with room aspect ratio.

ACKNOWLEDGEMENT

REFERENCES

1. T. Sakuma, "Approximate theory of reverberation in rectangular rooms with specular and diffuse reflections," J. Acoust. Soc. Am. **132**, 2325-2536 (2012).
2. D. Fitzroy, "Reverberation formula which seems to be more accurate with nonuniform distribution of absorption," J. Acoust. Soc. Am. **31**, 893-897 (1959).
3. J. Pujolle, "Nouvelle formule pour la durée de réverbération," ("New formula for the length of time of reverberation,") Rev. d'Acoust. **19**, 107-113 (1975).
4. Y. Hirata, "Geometrical acoustics for rectangular rooms," Acustica **43**, 247-252 (1979).
5. H. Arau-Puchades, "An improved reverberation formula," Acustica **65**, 163-179 (1988).
6. E. Nilsson, "Decay processes in rooms with non-diffuse sound fields," Report TVBA-1004, Lund Inst. Tech. (1992).
7. R. O. Neubauer, "Estimation of reverberation time in rectangular rooms with non-uniformly distributed absorption using a modified Fitzroy equation," Build. Acoust. **8**, 115-137 (2001).
8. M. Vorländer and E. Mommertz, "Definition and measurement of random-incidence scattering coefficients," Appl. Acoust. **60**, 187-200 (2000).
9. Y. Kosaka and T. Sakuma, "Numerical examination on the scattering coefficients of architectural surfaces using the boundary element method," Acoust. Sci. Tech. **26**, 136-144 (2005).
10. B. Dalenbäck, CATT-Acoustics v8 User's Manual, p.136, (2002).